

# NCAM-induced focal adhesion assembly: a functional switch upon loss of E-cadherin

Francois Lehembre<sup>1,5</sup>, Mahmut Yilmaz<sup>1</sup>,  
Andreas Wicki<sup>1</sup>, Tibor Schomber<sup>1</sup>,  
Karin Strittmatter<sup>1</sup>, Dominik Ziegler<sup>1</sup>,  
Angelika Kren<sup>1</sup>, Phillip Went<sup>2</sup>,  
Patrick WB Derksen<sup>3</sup>, Anton Berns<sup>4</sup>,  
Jos Jonkers<sup>3</sup> and Gerhard Christofori<sup>1,\*</sup>

<sup>1</sup>Department of Biomedicine, Institute of Biochemistry and Genetics, University of Basel, Basel, Switzerland, <sup>2</sup>Institute of Pathology, University of Basel, Basel, Switzerland, <sup>3</sup>Division of Molecular Biology, The Netherlands Cancer Institute, Amsterdam, The Netherlands and <sup>4</sup>Division of Molecular Genetics, The Netherlands Cancer Institute, Amsterdam, The Netherlands

**Loss of expression of the cell–cell adhesion molecule E-cadherin is a hallmark of epithelial–mesenchymal transition (EMT) in development and in the progression from epithelial tumours to invasive and metastatic cancers. Here, we demonstrate that the loss of E-cadherin function upregulates expression of the neuronal cell adhesion molecule (NCAM). Subsequently, a subset of NCAM translocates from fibroblast growth factor receptor (FGFR) complexes outside lipid rafts into lipid rafts where it stimulates the non-receptor tyrosine kinase p59<sup>Fyn</sup> leading to the phosphorylation and activation of focal adhesion kinase and the assembly of integrin-mediated focal adhesions. Ablation of NCAM expression during EMT inhibits focal adhesion assembly, cell spreading and EMT. Conversely, forced expression of NCAM induces epithelial cell delamination and migration, and high NCAM expression correlates with tumour invasion. These results establish a mechanistic link between the loss of E-cadherin expression, NCAM function, focal adhesion assembly and cell migration and invasion.**

*The EMBO Journal* (2008) 27, 2603–2615. doi:10.1038/emboj.2008.178; Published online 4 September 2008

**Subject Categories:** cell & tissue architecture; molecular biology of disease

**Keywords:** cancer; cell adhesion; E-cadherin; EMT; metastasis

## Introduction

When cancer cells disseminate from a primary tumour and infiltrate the surrounding tissue, they leave the tumour mass not only by gaining migratory and invasive capabilities but also by dissolving cell–cell contacts, known as tight and

adherens junctions (Friedl and Wolf, 2003). Consistent with this notion, the calcium-dependent cell–cell adhesion molecule E-cadherin, the prototype adhesion molecule of epithelial adherens junctions, is found absent or dysfunctional in the majority of epithelial cancers (carcinomas) (Cavallaro and Christofori, 2004). Inhibition of E-cadherin activity by specific neutralizing antibodies or shRNA-mediated down-regulation of its expression in epithelial MDCK cells leads to increased motility and invasiveness (Behrens *et al*, 1989; Qin *et al*, 2005). Conversely, the invasive behaviour of carcinoma cells can be blocked by forced expression of E-cadherin (Frixen *et al*, 1991). Using a transgenic mouse model of pancreatic  $\beta$ -cell carcinogenesis (Rip1Tag2), we have demonstrated earlier that the loss of E-cadherin is a rate-limiting event during tumour progression (Perl *et al*, 1998).

In many cancer types, the loss of E-cadherin coincides with a gain of expression of the mesenchymal cadherin, N-cadherin. This ‘cadherin switch’ is thought to be required for tumour cells to gain invasive properties (Cavallaro, 2004). Interestingly, the cadherin switch is also a hallmark of epithelial–mesenchymal transition (EMT), a process characterized by the combined loss of epithelial cell junction proteins, including E-cadherin,  $\alpha$ -catenin,  $\beta$ -catenin and claudins, and the gain of mesenchymal markers, such as N-cadherin, vimentin and fibronectin (Thiery, 2003; Thiery and Sleeman, 2006). EMT is a critical process during embryonic development and it is thought to have an important function in the progression of cancer, although this hypothesis is still under debate (Lee *et al*, 2006).

Here, we have investigated the functional consequences of the loss of E-cadherin in various cellular systems and transgenic mouse models and report that expression of the neuronal cell adhesion molecule (NCAM), a member of the immunoglobulin superfamily of genes, is upregulated concomitant with the loss of E-cadherin function. NCAM has been previously implicated in tumour progression and in lymph node metastasis, mainly by modulating  $\beta_1$ -integrin-mediated cell–matrix adhesion (Cavallaro *et al*, 2001; Christofori, 2003). In neurons, NCAM triggers distinct signal-transduction pathways. Within lipid rafts, NCAM associates with and activates p59<sup>Fyn</sup> kinase leading to the phosphorylation of focal adhesion kinase (FAK) and focal adhesion assembly, whereas in the non-raft compartment NCAM facilitates fibroblast growth factor receptor (FGFR)-activated signalling (Beggs *et al*, 1997; Niethammer *et al*, 2002). Here, we demonstrate that the upregulation of NCAM expression is a direct result of the loss of adherens junctions. As a consequence, NCAM clusters in lipid rafts together with p59<sup>Fyn</sup>, leading to FAK phosphorylation and focal adhesions assembly, activities required for cell motility and EMT.

## Results

### **EMT induced by the loss of E-cadherin**

We have employed several different experimental systems to investigate the functional impact of the loss of E-cadherin

\*Corresponding author. Department of Biomedicine, Institute of Biochemistry and Genetics, University of Basel, Mattenstrasse 28, 4058 Basel, Switzerland. Tel.: +41 61 267 3562; Fax: +41 61 267 3566; E-mail: gerhard.christofori@unibas.ch

<sup>5</sup>Present address: Actelion Pharmaceuticals Ltd, Allschwil, Switzerland

Received: 22 February 2008; accepted: 12 August 2008; published online: 4 September 2008

function on cell behaviour and cell signalling. First, TGF $\beta$  treatment of NMuMG murine mammary gland epithelial cells, a well-characterized EMT model, induced a loss of E-cadherin expression accompanied by a complete EMT (Miettinen *et al*, 1994; Bhowmick *et al*, 2001) (Figure 1A). Second, shRNA-mediated knock down of E-cadherin in MCF7 human epithelial breast carcinoma cells substantially reduced E-cadherin expression (MCF7-shEcad; Figure 1A and B). Third, genetic ablation of E-cadherin function was achieved by establishing a cell line from mammary tumours of MMTV-Neu transgenic mice (Muller *et al*, 1988), in which both E-cadherin alleles were flanked by LoxP recombination sites (MTflEcad cells) (Derksen *et al*, 2006). Expression of Cre-recombinase in MTflEcad cells led to a complete abrogation of E-cadherin expression (MTdeltaEcad; Figure 1A and B).

The lack of E-cadherin expression in both MCF7-shEcad and MTflEcad cells resulted in a loss of epithelial morphology and a gain of a fibroblast-like appearance (Figure 1A). Reduced expression of E-cadherin in MCF7 cells was accompanied by decreased expression of other epithelial markers, such as  $\beta$ -catenin, and an increased expression of the mesenchymal markers N-cadherin and vimentin. The lack of E-cadherin in MTflEcad cells induced only N-cadherin expression, without any upregulation of vimentin or loss of  $\beta$ -catenin (Figure 1B). Furthermore, MCF7-shEcad cells exhibited a eight-fold increase in cell motility and a three-fold increase in invasiveness, whereas MTdeltaEcad cells only displayed a 2.5-fold elevated motility but no increased invasiveness (Supplementary Figure S1A and B). These data indicate that removal of E-cadherin can induce either a *bona fide* EMT (MCF7-shEcad) or merely a 'cadherin-switch' in the absence of a full EMT (MTdeltaEcad). Notably, cell proliferation was diminished upon E-cadherin depletion in all experimental systems tested (Supplementary Figure S1C).

### EMT induces NCAM expression

Gene expression profiling experiments and quantitative RT-PCR analysis comparing NMuMG, MCF7 and MTflEcad cells before and after the loss of E-cadherin function revealed that the expression of NCAM was significantly upregulated upon loss of E-cadherin expression in TGF $\beta$ -treated NMuMG, MCF7-shEcad and MTdeltaEcad cells (Figure 1C). Immunoblotting analysis confirmed upregulated expression of the 140 kDa isoform of NCAM (NCAM140) in comparison to the E-cadherin-expressing cells (Figure 1B). NCAM mRNA upregulation was already detected 6 h after TGF $\beta$  treatment of NMuMG cells, and an increase in NCAM protein levels was observed 24 h after TGF $\beta$  treatment (Figure 1D and E), indicating that the upregulation of NCAM expression is an early event upon loss of E-cadherin function and EMT. Ablation of E-cadherin by treatment of MTflEcad cells with recombinant Cre recombinase protein carrying a HIV-Tat cell entry peptide resulted in the concomitant loss of E-cadherin expression with the gain of NCAM expression, demonstrating that NCAM expression is upregulated by the loss of E-cadherin without any additional TGF $\beta$  stimulation (Supplementary Figure S2B). Also in HEK293 cells, mesenchymal phenotype cells that expressed low levels of E-cadherin, shRNA-mediated ablation of E-cadherin expression resulted in an elongated cell shape with increased motility and an upregulation of NCAM expression (Supplementary Figure S3A–C).

Next, we investigated the effect of loss of E-cadherin expression on NCAM gene promoter activity by CAT reporter assays. Utilizing DNA sequences of the NCAM gene promoter region either 1 kb ( $\Delta$ Ssp) or 647 bp ( $\Delta$ Ndel) upstream of the transcriptional start site (Boras and Hamel, 2002), TGF $\beta$  treatment of NMuMG cells (Figure 1F) or ablation of E-cadherin expression in MCF7 cells (Supplementary Figure S2A) provoked a significant increase in NCAM promoter reporter activity. It has been recently reported that Smad4-depleted NMuMG cells (NMuMG-shSmad4) maintain an epithelial morphology upon TGF $\beta$  treatment (Deckers *et al*, 2006). Consistent with this report, NMuMG-shSmad4 cells still expressed high levels of E-cadherin after 3 days of TGF $\beta$  treatment, but only low levels of NCAM and N-cadherin in comparison to Smad4-expressing NMuMG-shControl cells (Figure 1G). These results indicate that Smad4-mediated signal transduction has a critical function in the induction of NCAM gene expression during TGF $\beta$ -induced EMT.

To investigate whether NCAM upregulation also occurs *in vivo*, we crossed mice carrying LoxP-flanked conditional alleles of the E-cadherin gene (Derksen *et al*, 2006) with Rip1Cre mice in which Cre-recombinase was specifically expressed in  $\beta$ -cells of the pancreatic islets of Langerhans (Ahlgren *et al*, 1998). Despite the low constitutive expression of NCAM in islet cells of normal control mice (Esni *et al*, 1999),  $\beta$ -cells that upon successful recombination had lost E-cadherin expression exhibited significantly higher levels of NCAM at their cell surface (Supplementary Figure S4). Taken together, these data indicate that the loss of E-cadherin causes increased NCAM gene expression *in vivo* and *in vitro*.

### NCAM is required for EMT

We next assessed whether increased NCAM levels were required for epithelial cells to undergo EMT. Three murine NCAM-specific siRNAs (simNCAM1, 2 and 3) efficiently downregulated NCAM mRNA and protein levels in NMuMG cells in comparison to control NCAM-mismatch-siRNA (siControl)-transfected cells (Figure 2A and B). NCAM-depleted NMuMG cells failed to undergo EMT and to upregulate the mesenchymal marker N-cadherin upon TGF $\beta$  treatment, whereas siControl-transfected NMuMG cells readily converted to mesenchymal cells, indicating that NCAM is required for EMT to occur (Figure 2A and C). Notably, ablation of NCAM expression in NMuMG cells, which after 13 days of TGF $\beta$  treatment had undergone full EMT, led to a reversion of EMT, with characteristic polarized epithelial cell morphology. This morphological change was accompanied by an increase in E-cadherin expression and a decrease in N-cadherin expression, demonstrating that NCAM is not only required for the initiation but also for the maintenance of EMT in NMuMG cells (Figure 2D).

To investigate the role of NCAM in tumours undergoing EMT *in vivo*, we analysed E-cadherin expression during tumour progression in the Rip1Tag2 (RT2) transgenic mouse model of pancreatic  $\beta$ -cell carcinogenesis (Hanahan, 1985), either wild type for NCAM expression or in a NCAM knockout background (RT2;NCAM+/+ and RT2;NCAM–/–, respectively; Perl *et al*, 1999). In wild-type RT2, the tumour areas showing downregulation of E-cadherin expression exhibited significantly higher intensities of diffuse NCAM-specific fluorescence staining at cell–cell contacts (Figure 2E). In

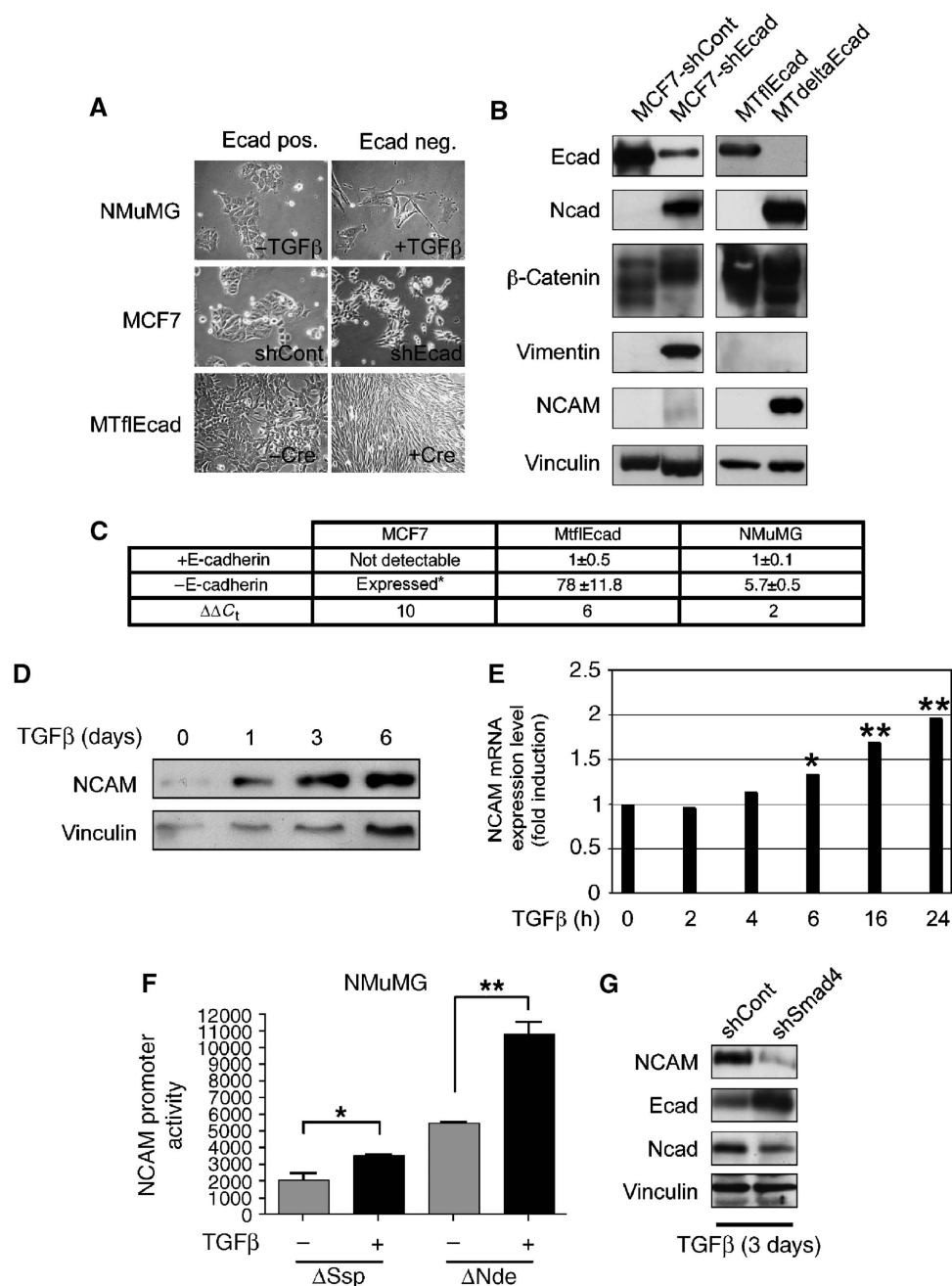


**Figure 1** E-cadherin loss in epithelial cell lines induces either a cadherin switch or full EMT. **(A)** NMuMG, MCF7 and MTF1Ecad cells adapt a mesenchymal phenotype upon loss of E-cadherin by TGFβ treatment (+ TGFβ), shRNA expression (shEcad) or Cre-mediated deletion of the *E-cadherin* gene (+ Cre). **(B)** Immunoblot analysis for E-cadherin (Ecad), N-cadherin (Ncad), β-catenin, vimentin and NCAM expression in MCF7 and MTF1Ecad cells expressing E-cadherin (shCont and MTF1Ecad) or depleted for E-cadherin expression by shRNA expression (shEcad) or Cre-mediated deletion of the E-cadherin locus (MTdeltaEcad). Cell extracts were loaded on different gels and resolved proteins were visualized with specific antibodies as indicated. Immunoblotting for vinculin was used as a loading control. **(C)** NCAM expression is induced upon loss of E-cadherin function. NCAM mRNA levels were determined by quantitative RT-PCR in MCF7, MTF1Ecad and NMuMG cells that have been depleted for E-cadherin (-E-cadherin) or not (+E-cadherin). For all values  $P < 0.0001$ , unpaired *t*-test. Data are shown as mean ± s.d. \*As NCAM is not expressed at detectable levels in MCF7 cells, its upregulated expression in MCF7-shEcad cells cannot be calculated as fold induction. Instead the comparative  $C_t$  values ( $\Delta\Delta C_t$ ) are given in the lower row. **(D)** Immunoblot analysis for NCAM protein expression in NMuMG cells in the presence of TGFβ at the indicated time points. Immunoblotting for vinculin was used as a loading control. **(E)** NCAM mRNA levels were determined by quantitative RT-PCR in NMuMG cells treated with TGFβ for the times indicated. \* $P = 0.0134$ , \*\* $P < 0.005$ ; unpaired *t*-test). Data are shown as mean ± s.d. **(F)** NCAM promoter activity is increased upon loss of E-cadherin expression. NMuMG were transfected with a CAT reporter plasmid containing 1000 bp ( $\Delta Ssp$ ) or 647 bp ( $\Delta Nde$ ) of the NCAM promoter sequence and treated with or out TGFβ for 6 days prior to the analysis of CAT activity (left panel; \* $P = 0.0027$  and \*\* $P = 0.0007$ , unpaired *t*-test). Data are shown as mean ± s.d. **(G)** NMuMG cells stably transfected with shControl or shSmad4 were treated for 3 days with TGFβ and then analysed for NCAM, E-cadherin (Ecad) and N-cadherin (Ncad) expression by immunoblotting analysis. Immunoblotting for vinculin was used as a loading control.

contrast, in the absence of NCAM expression, 75% of the invasive carcinomas of RT2;NCAM<sup>-/-</sup> mice showed high levels of E-cadherin expression (Figure 2F;  $P < 0.0001$ ,

Fisher's exact test). Altogether, these results indicate that ablation of NCAM expression prevents EMT and E-cadherin loss *in vitro* and *in vivo*.

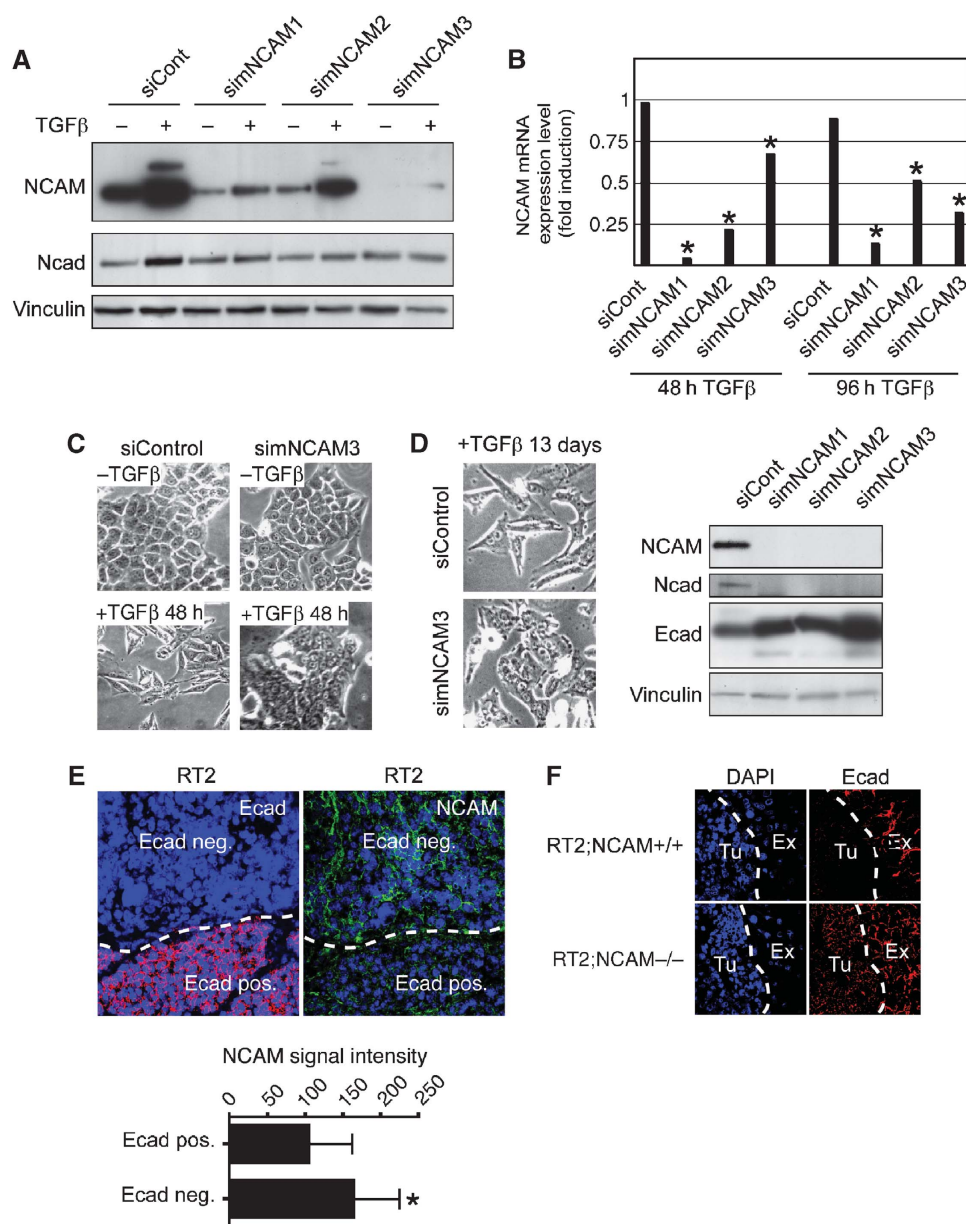


**Figure 2** NCAM is required for EMT. (A) Immunoblot analysis of NCAM and N-cadherin (Ncad) in siControl (siCont) and simNCAM-transfected NMuMG cells. At 24 h after transfection, TGFβ was added to the medium for 48 h. Immunoblotting for vinculin was used as a loading control. (B) Levels of NCAM mRNA were determined by quantitative RT-PCR in NMuMG cells that have been transfected with siControl and simNCAM for 24 h before treatment with TGFβ for 48 or 96 h. For all values,  $*P < 0.002$  compared with siControl-transfected cells, unpaired *t*-test. Data are shown as mean  $\pm$  s.d. (C) Phase-contrast microscopy of siControl and simNCAM-transfected NMuMG cells treated with or without TGFβ for 48 h. (D) NMuMG cells were treated for 13 days with TGFβ before transfection of a control (siControl) and or an NCAM-specific siRNA (simNCAM3). After 48 h, phase-contrast images were taken (left panels). NCAM, N-cadherin (Ncad) and E-cadherin (Ecad) expression levels were analysed by immunoblotting (right panel). Antibodies against vinculin were used as a loading control. (E) Immunofluorescence staining for E-cadherin (red) and NCAM (green) on pancreatic sections from Rip1Tag2 mice. Lower panel: quantification of NCAM fluorescence in cell-cell junctions from E-cadherin-positive cells or E-cadherin-negative cells (each  $n = 40$ ) shows increased expression in cells that have lost E-cadherin ( $*P < 0.0001$ , unpaired *t*-test). Blue DAPI staining visualizes nuclei. (F) Immunofluorescence staining for E-cadherin (red) on pancreatic sections from Rip1Tag2;NCAM+/+ (upper panels), Rip1Tag2;NCAM-/- (lower panels) and Rip1Tag2 mice (right panels). Note that in contrast to carcinomas of Rip1Tag2;NCAM+/+ mice, E-cadherin expression is maintained in carcinomas of Rip1Tag2;NCAM-/- mice. Blue DAPI staining visualizes nuclei. Ex, exocrine tissue; Tu, tumour tissue.

### NCAM is sufficient to induce hallmarks of EMT

We next examined whether NCAM was able to induce EMT in epithelial cells. Ectopic expression of NCAM induced cell death in NMuMG as well as in MCF7 cells, as reported earlier with other EMT regulators (Mani *et al*, 2007). We thus established several independent clones of MDCK epithelial cells expressing NCAM140 (Figure 3A). Notably, NCAM-expressing MDCK cells formed numerous foci on top of the

confluent cell monolayer, a feature that was not observed in control-transfected cells (Figure 3B). Under sparse conditions, NCAM-expressing cells scattered and did not form cell-cell contacts, whereas control MDCK cells formed small cell clusters (Figure 3B).

In heterogeneous populations of NCAM-expressing and non-expressing cells, the majority of the NCAM-expressing cells delaminated from the cellular monolayer and migrated



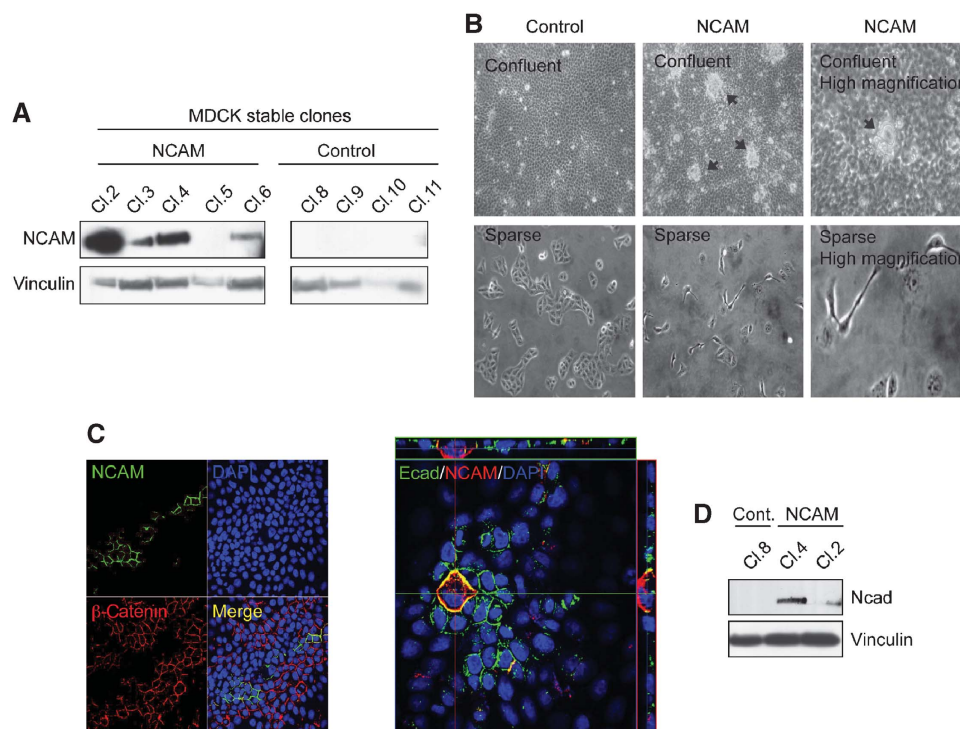


**Figure 3** NCAM induces partial EMT. **(A)** Immunoblotting analysis of NCAM expression in MDCK cell clones either transfected with empty vector (control) or with an NCAM expression vector (NCAM). Immunoblotting for vinculin was used as a loading control. **(B)** Phase-contrast microphotographs of confluent (upper panels) and sparse (lower panels) MDCK clones expressing NCAM (NCAM) or not (control). Arrows indicate foci of cells growing on top of the cell monolayer. **(C)** Confocal laser scanning microscopy analysis of NCAM,  $\beta$ -catenin and E-cadherin (Ecad) expression in a mixture of MDCK cells expressing NCAM or not. Note that the NCAM expressing cells (green) do not express  $\beta$ -catenin (red) on their cell surface (left panel). The right panel shows a single NCAM-expressing cell that has lost E-cadherin expression and delaminates and migrates on top of the confluent, E-cadherin-expressing cell monolayer, as illustrated by the z-axis above and on the right side of the panel. **(D)** Immunoblot analysis of N-cadherin (Ncad) in MDCK cells stably expressing NCAM. Immunoblotting against vinculin was used as a loading control.

on top of neighbouring epithelial cells (Figure 3C). In the NCAM-expressing cells, adherens junction proteins, such as  $\beta$ -catenin and E-cadherin, were undetectable (Figure 3C), whereas N-cadherin expression was increased (Figure 3D). These results indicate that NCAM is able to induce morphological and molecular changes representing typical hallmarks of EMT in MDCK cells (shown here) and also in E-cadherin-transfected fibroblastoid L cells (Esni *et al*, 1999).

#### NCAM induces focal adhesion assembly

As we had shown earlier that NCAM was able to modulate  $\beta_1$ -integrin-mediated cell-matrix adhesion (Cavallaro *et al*, 2001), we compared control- and NCAM-depleted cells for their ability to spread on fibronectin-coated culture dishes. Cell spreading was significantly reduced in TGF $\beta$ -treated NMuMG cells upon NCAM removal (Figure 4A and B). Furthermore, cell spreading of TGF $\beta$ -treated, 'mesenchymal' NMuMG cells could be repressed by neutralizing antibodies against  $\beta_1$ -integrin (Figure 4A), whereas spreading of non-treated epithelial NMuMG cells was unaffected (Figure 4B). Consistent with this notion, numerous focal contacts were observed at the ventral surface of TGF $\beta$ -treated NMuMG cells in comparison to their epithelial counterparts (Figure 4C), and cells undergoing EMT exhibited increased amounts of phosphorylated FAK and paxillin and enhanced cell spreading (Figure 4D). Such TGF $\beta$ -mediated focal adhesion assembly as well as FAK phosphorylation was not observed in

NCAM-depleted NMuMG cells (Figure 4C and D). In a time course of mesenchymal cell spreading, FAK was constantly phosphorylated, suggesting a high stability of the focal adhesions, whereas in NCAM-depleted cells, the levels of FAK phosphorylation oscillated, indicating a high turnover of focal adhesions (Figure 4E).

Transwell migration assays revealed a significantly higher chemotactic migration of TGF $\beta$ -treated, simNCAM-transfected NMuMG cells as compared with TGF $\beta$ -treated, siControl-transfected cells (Figure 4F). Moreover, NCAM-depleted TGF $\beta$ -treated NMuMG cells migrated significantly faster in scratch wounding assays than NCAM-expressing control cells (Supplementary Figure S5). However, adhesion assays performed to quantify stable matrix attachment of cells independent of their spreading capacity did not reveal any differences between NCAM-expressing and non-expressing cells (data not shown). These data suggest that NCAM has a critical function in focal adhesion assembly and turnover, rather than in modulating the strength of cell-matrix adhesion.

#### NCAM re-localizes into lipid rafts upon EMT

In neurons, it has been reported that a signalling complex between NCAM, p59<sup>Fyn</sup> and FAK is formed upon homophilic NCAM-NCAM interactions, and that NCAM-mediated signalling through p59<sup>Fyn</sup> depends on its localization to lipid rafts (Beggs *et al*, 1997; Niethammer *et al*, 2002). Indeed, TGF $\beta$  treatment of NMuMG cells led to increased phosphorylation

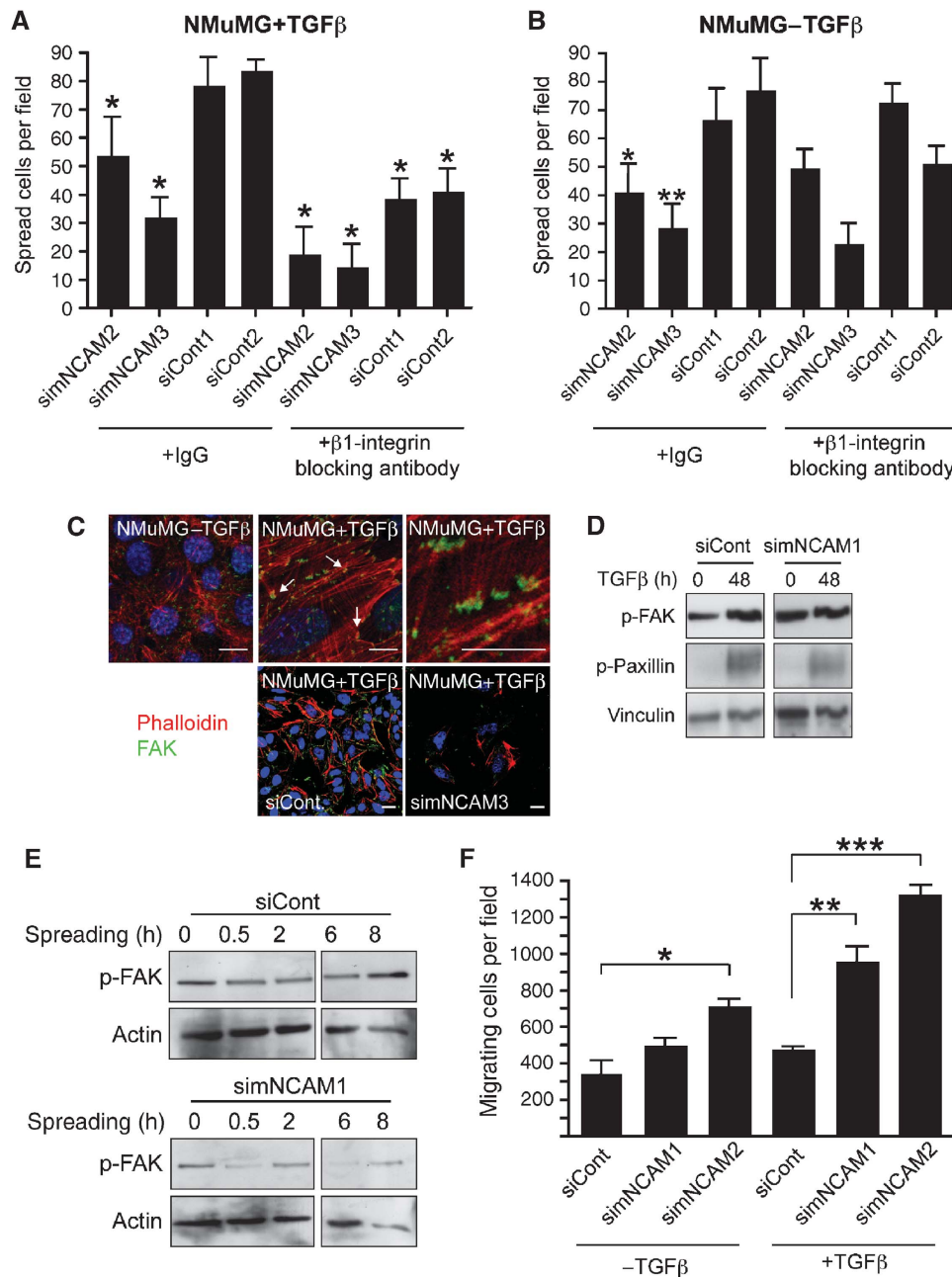


**Figure 4** NCAM is required for focal adhesion assembly during EMT. (A, B) TGF $\beta$ -treated NMuMG cells show a markedly reduced cell spreading upon siRNA-mediated depletion of NCAM expression (simNCAM) as compared with control-treated cells (siCont). Cell spreading is further reduced by the addition of neutralizing antibodies against  $\beta_1$ -integrin in TGF $\beta$ -treated NMuMG cells (A) but not in untreated cells (B). Data are shown as mean  $\pm$  s.d. \* $P$  < 0.05, unpaired  $t$ -test. (C) Immunofluorescence staining for actin (red) and p125<sup>FAK</sup> (green) in NMuMG cells in the presence or absence of TGF $\beta$ , as indicated. Numerous focal adhesions are detected in TGF $\beta$ -treated cells (arrows, middle upper panel) as compared with control cells (left panel). Higher magnification of the middle upper panel is shown on the right. Lower panels: NCAM depletion leads to impaired focal adhesion assembly in siCont- and simNCAM-treated NMuMG cells treated with TGF $\beta$ . Staining with DAPI (blue) visualizes nuclei. Size bars = 10  $\mu$ m. (D) Immunoblotting analysis of NMuMG cells reveals an increase in FAK and paxillin phosphorylation upon EMT induction (left panel). Treatment with siRNA against murine NCAM (simNCAM1, right panel) represses the increase in EMT-induced FAK phosphorylation as observed in control-treated cells (siCont; left panel). Immunoblotting for vinculin was used as a loading control. (E) TGF $\beta$ -treated NMuMG cells were transfected with control siRNA (siCont) or with siRNA targeting NCAM expression (simNCAM1), allowed to spread on the culture dish for the indicated time points and levels of FAK phosphorylation were determined by immunoblotting with antibodies specifically recognizing phosphorylated FAK. Immunoblotting for actin was used as a loading control. (F) Depletion of NCAM expression (simNCAM) significantly induces migration of NMuMG cells through Transwell filters as compared with control-siRNA-treated cells (siControl). \* $P$  = 0.043, \*\* $P$  = 0.013, \*\*\* $P$  = 0.0024, unpaired  $t$ -test. Data are shown as mean  $\pm$  s.d.

of p59<sup>Fyn</sup> (Figure 5A). Immunofluorescence analysis revealed that in TGF $\beta$ -treated NMuMG cells, NCAM was predominantly localized in the junctions between cells and in focal plasma membrane areas (Figure 5B, upper panels) where it colocalized with FAK (Figure 5B, lower panels). Sucrose

gradient density centrifugation experiments demonstrated that the low levels of NCAM present in epithelial NMuMG cells were found exclusively in the detergent-soluble protein fractions (Figure 5C). In contrast, in TGF $\beta$ -treated NMuMG cells, a substantial proportion of the high levels of NCAM

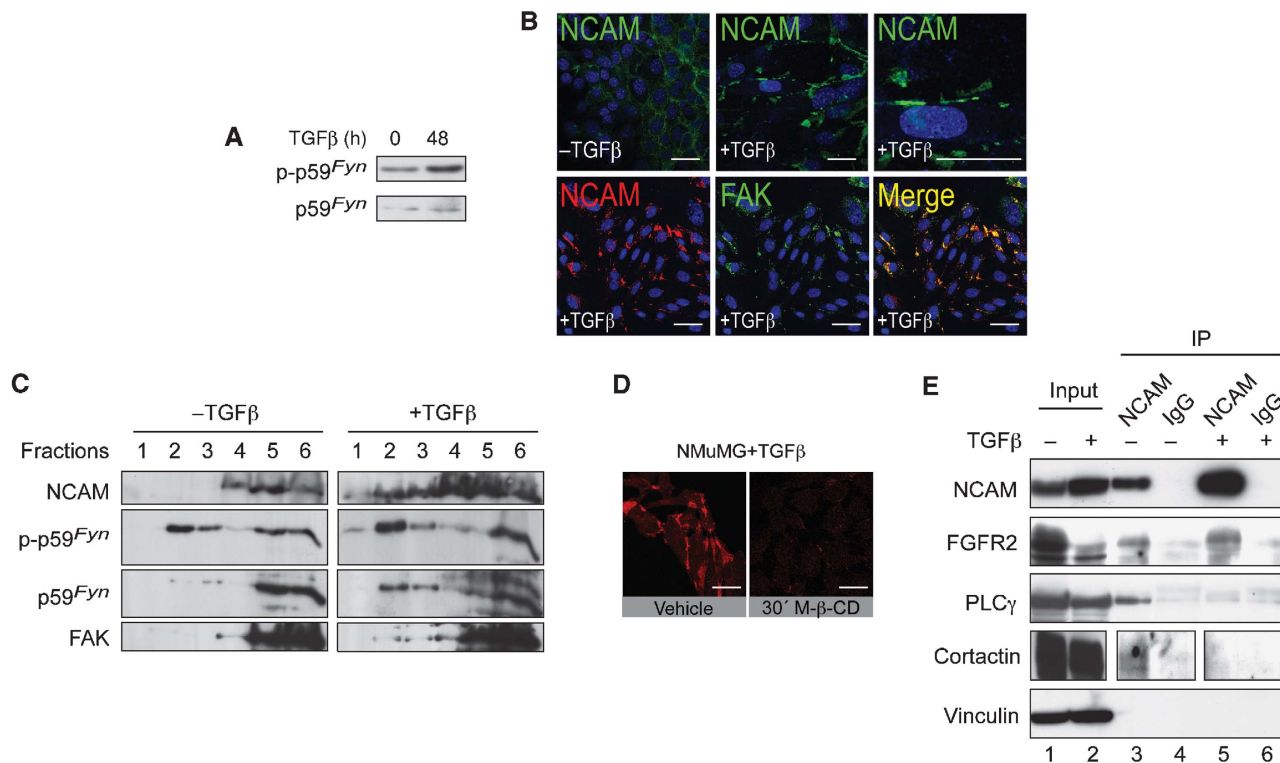


**Figure 5** During EMT, NCAM localizes into lipid rafts together with p59<sup>Fyn</sup> and FAK. (A) Immunoblotting analysis of NMuMG cells reveals an increase in p59<sup>Fyn</sup> phosphorylation upon EMT induction (+ TGFβ). Immunoblotting for total p59<sup>Fyn</sup> was used as a loading control. (B) Upper panels: Immunofluorescence staining for NCAM (green) in NMuMG cells in the presence or absence of TGFβ. During EMT, NCAM is translocated from sites of cell–cell contacts to foci at the plasma membrane (see higher magnification in top right panel). Lower panels: NCAM (red) and FAK (green) colocalize in TGFβ-treated NMuMG cells. DAPI staining (blue) visualizes nuclei. Size bars = 20 μm. (C) NCAM140 associates with lipid rafts upon induction of EMT. Lysates of TGFβ-treated or non-treated NMuMG cells were fractionated by sucrose gradient centrifugation and proteins were resolved by SDS gel electrophoresis. After blotting, membranes were cut into upper and lower halves. The upper half was sequentially probed with antibodies against NCAM and FAK, the lower half was probed with antibodies against phosphorylated-p59<sup>Fyn</sup> and total p59<sup>Fyn</sup>. In mesenchymal cells (+ TGFβ), NCAM, p59<sup>Fyn</sup> and FAK are present in lipid rafts (lanes 1–3) as well as in the Triton X-100-soluble high-density fractions (lanes 4–6). In epithelial cells (–TGFβ), they are detected only in the high-density fractions (lanes 4–6). (D) Immunofluorescence staining of NCAM (red) in NMuMG cells treated with TGFβ. Upon methyl-β-cyclodextrin (M-β-CD) treatment, lipid rafts are disorganized and NCAM clusters disappear. Size bars = 20 μm. (E) NCAM forms a complex with FGFR2, PLCγ and cortactin in epithelial cells. Lysates from NMuMG cells treated with or without TGFβ were immunoprecipitated with anti-NCAM antibodies (NCAM) or unrelated isotype immunoglobulin (IgG). Total lysates and immunoprecipitates were resolved by SDS gel electrophoresis, and after protein transfer the blot was sequentially probed with antibodies specific for PLCγ, NCAM, FGFR2 and vinculin. Cortactin was probed on a separate blot from a gel loaded with the same experimental cell extracts. Note that NCAM precipitates PLCγ and cortactin only in untreated NMuMG cells but not in TGFβ-treated cells.

were also detected in the top fractions of the gradient (Figure 5C), indicating an association of NCAM with detergent-resistant lipid rafts. FAK and phosphorylated p59<sup>Fyn</sup> were also found in the NCAM-containing lipid raft fractions of the gradient. Disruption of lipid rafts by cholesterol depletion with methyl-β-cyclodextrin (M-β-CD) completely impaired the formation of NCAM clusters in TGFβ-treated NMuMG cells, whereas the actin cytoskeleton and cell shape remained largely unaffected (Figure 5D, data not shown). These experiments indicate that a subset of NCAM shifts its localization to p59<sup>Fyn</sup>/FAK containing lipid rafts upon the transition to a mesenchymal phenotype.

As NCAM has been shown to physically associate with FGFR, PLCγ and cortactin outside lipid rafts (Cavallaro *et al*, 2001), we next assessed whether these NCAM-containing signalling complexes were unchanged during EMT. Immunoprecipitation experiments with antibodies against NCAM revealed that FGFR2 was found associated with NCAM regardless of TGFβ treatment of NMuMG cells. In contrast, the signalling effectors PLCγ and cortactin co-im-

munoprecipitated with NCAM exclusively in untreated epithelial NMuMG cells and not in TGFβ-treated ‘mesenchymal’ NMuMG cells (Figure 5E). These data suggest that during TGFβ-induced EMT of NMuMG cells, NCAM changes its subcellular localization and its signalling partners, which in turn leads to focal adhesion stabilization.

#### NCAM mediates focal adhesion assembly in various EMT systems

To assess whether NCAM exerts this critical function also during EMT in other experimental systems, its expression was ablated in MCF7-shEcad, MTdeltaEcad and HEK293 cells by transfection of specific murine or human siRNAs (Supplementary Figure S6A–D). In MCF7-shEcad cells depleted from NCAM, a loss of neurite extensions was observed (Figure 6A), an established hallmark of NCAM function (Cavallaro *et al*, 2001). In contrast, no obvious morphological changes were observed in MTdeltaEcad cells upon NCAM depletion (data not shown), suggesting that these cells were irreversible in their mesenchymal phenotype



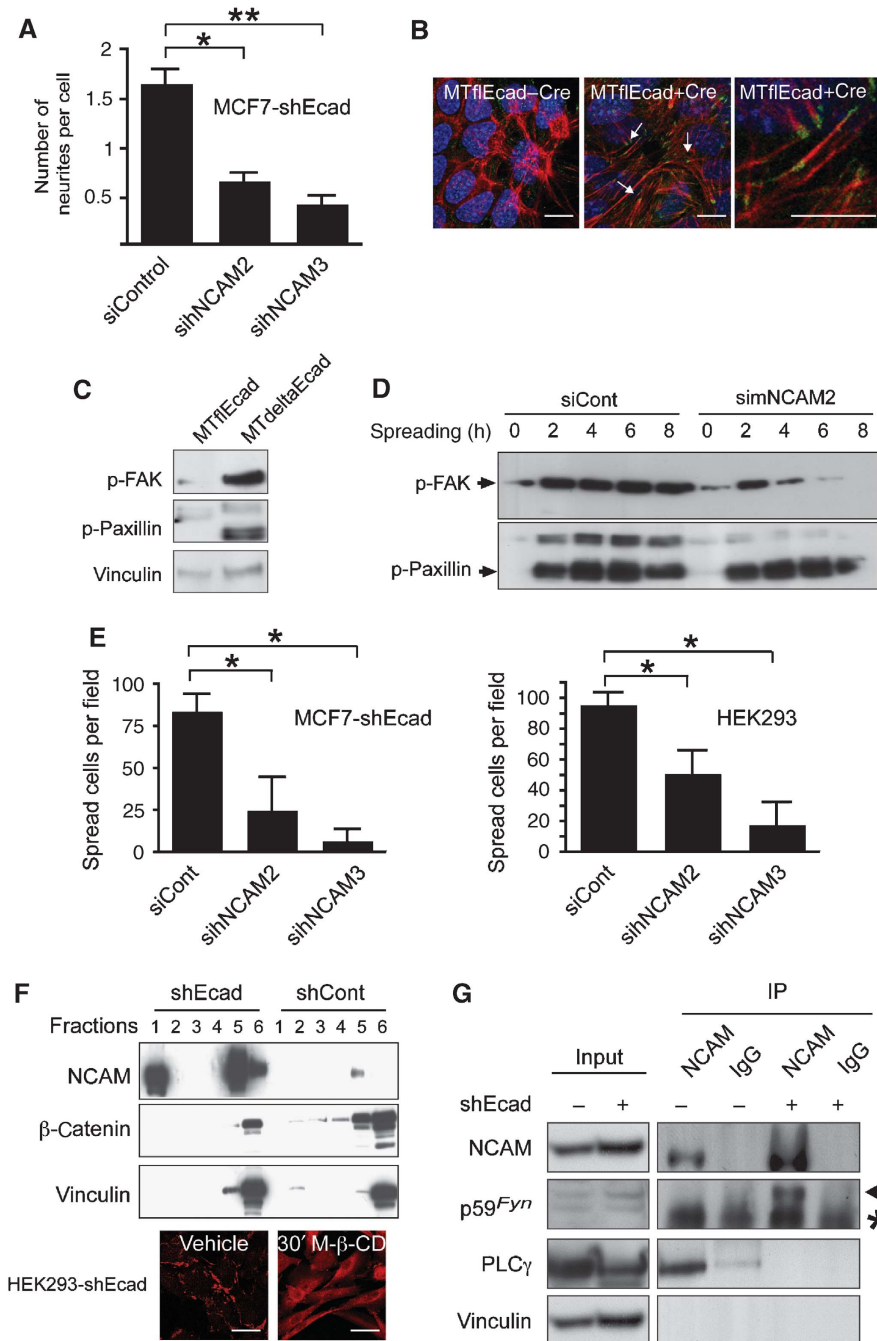


**Figure 6** NCAM expression controls focal adhesion assembly in various mesenchymal cells. **(A)** Quantification of neurites in MCF7-shEcad cells reveals that the number of neurites per cell is significantly decreased in simNCAM-transfected cells compared with siControl-transfected cells (lower panel,  $*P = 0.0133$  and  $**P = 0.0087$ , unpaired *t*-test). Data are shown as mean  $\pm$  s.d. **(B)** Immunofluorescence staining for actin (red) and p125<sup>FAK</sup> (green) on MTflEcad cells with and without Cre-recombinase expression. Numerous focal adhesions are detected in E-cadherin-depleted cells (arrows, middle panel) as compared with control cells (left panel). Higher magnification of the middle panel is shown on the right. Staining with DAPI (blue) visualizes nuclei. Size bars = 10  $\mu$ m. **(C)** Immunoblotting analysis of MTflEcad and MTdeltaEcad cells reveals an increase in FAK and paxillin phosphorylation upon mesenchymal transition. Immunoblotting for vinculin was used as a loading control. **(D)** MTdeltaEcad cells were transfected with siControl or simNCAM siRNA, allowed to spread for the indicated times and the levels of phosphorylation of FAK and paxillin were determined by immunoblotting analysis. Cell lysates were resolved by SDS gel electrophoresis, and after protein transfer blots were sequentially probed with antibodies against phosphorylated FAK and phosphorylated paxillin. **(E)** Cell spreading of MCF7-shEcad and HEK293 cells transfected with different siRNAs targeting NCAM (sihNCAM2 and 3) on plastic culture dishes is reduced as compared with control-treated cells (siCont).  $*P = 0.0021$ , unpaired *t*-test. Data are shown as mean  $\pm$  s.d. **(F)** NCAM140 associates with lipid rafts upon loss of E-cadherin expression. Upper panels: lysates of HEK293-shEcad and HEK293-shCont cells were fractionated by sucrose gradient centrifugation and analysed by immunoblotting for NCAM,  $\beta$ -catenin and vinculin as a loading control. In E-cadherin-depleted cells (shEcad), NCAM is present in lipid rafts (fractions 1 and 2) as well as in the Triton X-100-soluble high-density fractions (fractions 5 and 6). In the presence of E-cadherin (shCont), NCAM is detected only in the high-density fractions (fractions 5 and 6). Lower panels: immunofluorescence staining of NCAM (red) in HEK293-shEcad cells treated with methyl- $\beta$ -cyclodextrin (M- $\beta$ -CD). Upon treatment, lipid rafts are disorganized and NCAM clusters disappear. Size bars = 20  $\mu$ m. **(G)** HEK293-shEcad (shEcad+) and HEK293-shCont (shEcad-) cell lysates were immunoprecipitated with antibodies against NCAM or an unrelated immunoglobulin (IgG) isotype. NCAM precipitated p59<sup>Fyn</sup> (arrow) only in the absence of E-cadherin, and PLC $\gamma$  only in the presence of E-cadherin. Vinculin was used as a loading control. The asterisk indicates immunoglobulin heavy chain.



(note that these cells carry an irreversible deletion of the *E-cadherin* gene).

As observed in TGF $\beta$ -treated NMuMG cells, numerous focal contacts were observed at the ventral surface of MTdeltaEcad and MCF7-shEcad cells (Figure 6B and data not shown). Consistent with this observation, increasing amounts of phosphorylated FAK and paxillin were observed in cells in MTdeltaEcad in comparison to their epithelial counterparts (Figure 6C). Upon depletion of NCAM from MTdeltaEcad cells, FAK phosphorylation was rapidly lost during cell spreading, whereas it remained constant in control cells (Figure 6D). As a consequence, cell spreading of NCAM-depleted MCF7-shEcad, MTdeltaEcad and HEK293 cells were reduced (Figure 6E and data not shown). Notably, phosphorylation of paxillin was unaffected by the presence or absence of NCAM, indicating that paxillin phosphorylation is mediated by an NCAM-independent pathway (Figures 4C and D, and 6D).

Comparable to NMuMG cells, in HEK293 cells, NCAM localization also shifted from non-lipid raft to lipid raft membrane fractions upon loss of E-cadherin (Figure 6F). Consistent with this observation, disruption of lipid rafts by cholesterol depletion with M- $\beta$ -CD completely impaired the formation of NCAM clusters in HEK293-shEcad and MTdeltaEcad cells (Figure 6F and data not shown). Forced, inducible expression of NCAM in HEK293 cells resulted in the translocation of a subset of NCAM into lipid rafts, demonstrating that increased levels of NCAM protein mediate its translocation to lipid rafts and that the loss of E-cadherin is not necessarily required for this process (Supplementary Figure S7).

Immunoprecipitation experiments revealed that in E-cadherin-deficient HEK293-shEcad cells, the high levels

of NCAM associated with p59<sup>Fyn</sup>, an interaction that could not be detected in control cells expressing low levels of NCAM (Figure 6G). Similar to TGF $\beta$ -treated NMuMG cells, in HEK293 cells NCAM associated with PLC $\gamma$  only in the presence of E-cadherin (Figure 6G). These results indicate that, upon loss of E-cadherin function, NCAM ceases to associate with PLC $\gamma$  and cortactin and a subset of NCAM protein re-localizes to lipid rafts where it binds to p59<sup>Fyn</sup>.

### Expression of NCAM in human and mouse tumours

We next determined whether upregulated NCAM expression was also observed in E-cadherin-negative cancer cells *in vivo*. NCAM and E-cadherin expression were analysed by immunohistochemical staining of tumour tissue from a recently published mouse model of lobular breast carcinogenesis, in which mice carrying LoxP-flanked alleles of the p53 gene (Trp53F) were crossed with keratin14 gene promoter-Cre recombinase mice (K14-Cre) and with mice carrying LoxP-flanked alleles of E-cadherin (EcadF/F; Derksen *et al*, 2006). In E-cadherin-expressing tumours (K14-Cre;Trp53F/F;EcadF/+), E-cadherin was expressed at the membrane of most tumour cells (Figure 7A), whereas NCAM could only be detected in large blood vessels of the surrounding fat or muscle tissue and in the basal layer of the epidermis (Figure 7A,b). In contrast, in tumours of K14-Cre;Trp53F/F;EcadF/F mice, E-cadherin expression was efficiently ablated (Figure 7A,c), yet NCAM expression was now detectable at varying intensities in tumour cells (Figure 7A,d). In particular, cells within invasive tumour fronts displayed significant NCAM expression, for example at the interface between tumours and subcutaneous myocytes and

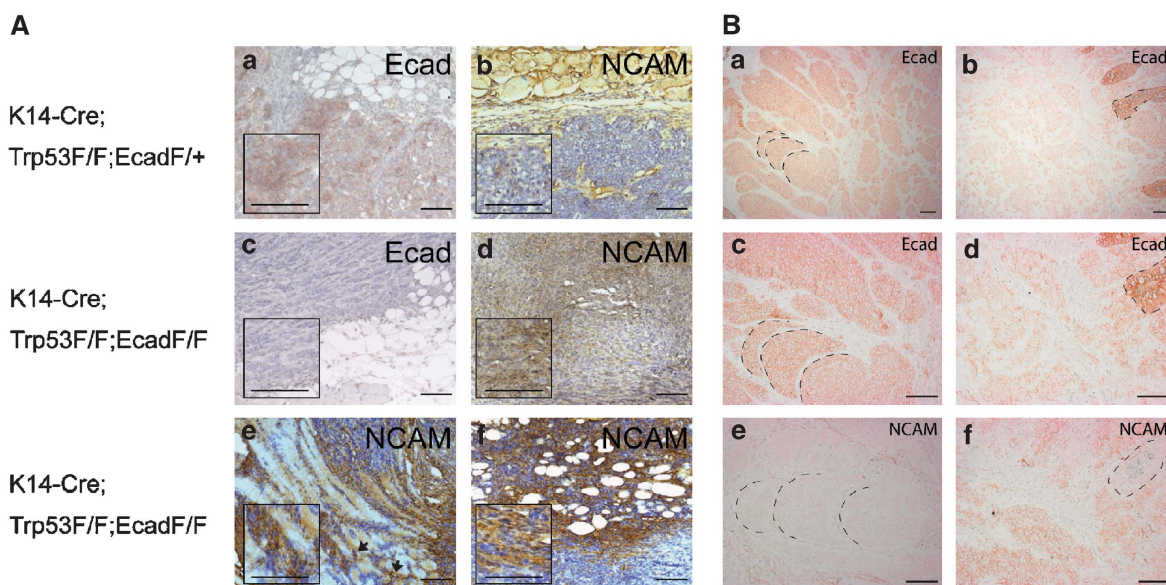


**Figure 7** NCAM is upregulated in E-cadherin-negative tumours. (A) Serial histological sections from breast tumours of K14-Cre;Trp53F/F mice expressing E-cadherin (Ecad F/+ ) or deficient in E-cadherin expression (Ecad F/F) were stained with antibodies against E-cadherin (a, c) and NCAM (b, d–f). NCAM is absent in E-cadherin-expressing tumour cells (a, b). In contrast, NCAM is expressed in tumours that have lost E-cadherin expression (c, d). NCAM is predominantly expressed on the invasive front of E-cadherin-negative tumours at the interphase between tumour cells and myocytes (e) or adipocytes of the skin (f). Disseminated tumour cells in the stroma (indicated by arrows in e) also display strong NCAM staining. Inserts represent higher magnifications of the respective sections. Size bars = 100  $\mu$ m. (B) Serial histological sections from a human patient neuroendocrine carcinoid were stained with antibodies against E-cadherin (a–d) and NCAM (e, f). NCAM is not expressed in E-cadherin-positive, differentiated cancer cells, whereas NCAM is expressed in invasive cancer cells with reduced E-cadherin expression. Morphological structures are marked for orientation. Size bars = 200  $\mu$ m.

adipocytes, as well as in disseminated tumour cells (Figure 7A,e and f).

We next assessed NCAM expression in human cancers by immunohistochemical staining of multi-tissue arrays containing 39 different human cancer types and corresponding 22 normal tissues. Depending on availability, between 5 and 50 samples per cancer type were analysed. A particular strong upregulation of NCAM was observed in neuroendocrine tumours, including small-cell lung cancer (35 of 43 patients,  $P < 0.001$ , Fisher's exact test) and intestinal carcinoids (33 of 44 patients,  $P < 0.001$ , Fisher's exact test), cancer types known to lose E-cadherin expression during tumour progression (Salon *et al*, 2004). Staining of serial histological sections of a human intestinal neuroendocrine carcinoid revealed expression of NCAM predominantly in the invasive cancer cells of the tumour with low or no E-cadherin expression, whereas NCAM was not found to be expressed in the E-cadherin positive, differentiated compartments of the tumour (Figure 7B). These results indicate that NCAM is upregulated upon loss of E-cadherin function in certain types of human cancers.

## Discussion

We have employed cellular experimental systems, transgenic mouse models and patient biopsies to investigate how the loss of E-cadherin function contributes to tumour progression. Notably, E-cadherin depletion in cultured cells *in vitro* leads to increased expression of the cell adhesion molecule NCAM. A comparable NCAM upregulation is also observed in transgenic mouse models of malignant insulinoma and lobular breast carcinoma and in human small-cell lung cancer

and intestinal carcinoids, where a loss of E-cadherin and a gain of mesenchymal markers have been previously implicated in tumour progression (Perl *et al*, 1998; Salon *et al*, 2004; Derksen *et al*, 2006, this paper). Interestingly, expression of L1, a close relative of NCAM, is also observed in E-cadherin-negative cells of the invading tumour front, for example in colorectal cancer (Gavert *et al*, 2005).

The molecular mechanisms underlying the regulation of NCAM gene expression during EMT are the focus of intense investigations in our laboratory. Here, we have assessed the functional contribution of upregulated NCAM expression to EMT. In the tumour progression models employed here, NCAM is found in two distinct complexes: in the presence of E-cadherin, low levels of NCAM localize outside lipid rafts and associate with FGFR, PLC $\gamma$  and cortactin. Upon loss of E-cadherin function, NCAM expression levels are increased, and a subset of NCAM protein translocates to lipid rafts, where it associates with p59<sup>Fyn</sup>. Subsequent phosphorylation and activation of p59<sup>Fyn</sup> and its effector substrate FAK result in the stabilization of  $\beta_1$ -integrin-mediated focal adhesions and increased cell spreading and migration (Figure 8). On the other hand, FGFR transmits NCAM-dependent and NCAM-independent signals: NCAM-mediated activation of FGFR leads to the activation of PLC $\gamma$  and through the Raf-kinase PKC $\beta_{II}$  to sustained MAPK activation and increased cell adhesion. In contrast, stimulation of FGFR by FGFs activates PLC $\gamma$ /PKC $\alpha$  and Ras/Raf/MAPK signalling pathways and promotes cell adhesion and proliferation (Francavilla *et al*, 2007; Figure 8). Thus, loss of E-cadherin affects the nature of NCAM-mediated signal transduction by inducing NCAM gene expression and by changing NCAM's subcellular localization. Forced expression of NCAM also resulted in its translocation to lipid rafts even in

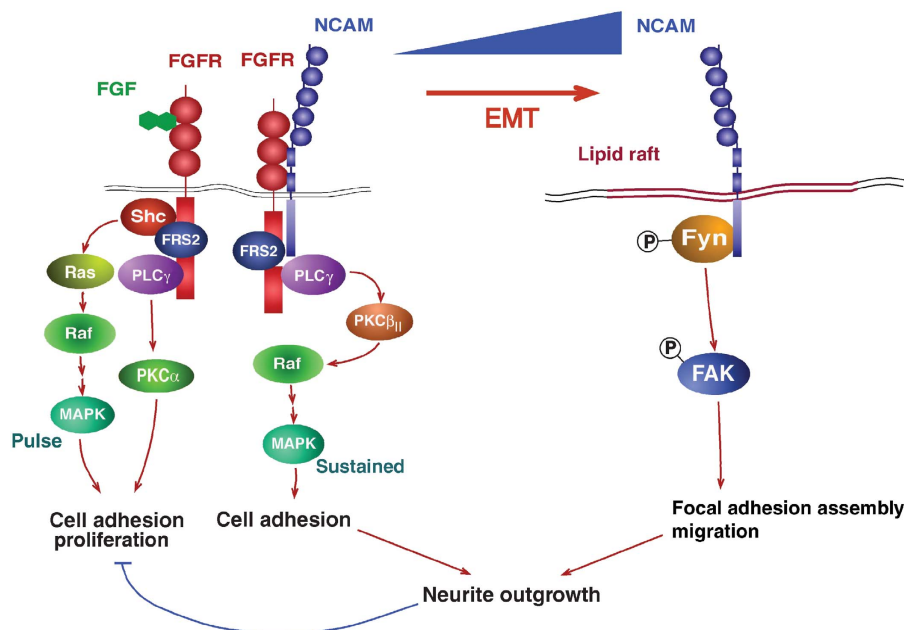


**Figure 8** NCAM upregulation leads to a functional switch. A working model of the molecular mechanisms underlying the change in NCAM subcellular localization and its interacting partners during EMT is depicted. In epithelial cells, low levels of NCAM form a complex with FGFR and PLC $\gamma$  leading to the activation of the Raf-kinase PKC $\beta_{II}$  and thus to a sustained activation of the MAPK pathway and cell adhesion. Upon loss of E-cadherin function during EMT, NCAM is highly expressed, and a subset localizes to lipid rafts where it associates with p59<sup>Fyn</sup>, leading to FAK phosphorylation, focal adhesion assembly and cell migration. Both NCAM-mediated signalling pathways are required for neurite outgrowth. In contrast, FGF-induced stimulation of FGFR results in PLC $\gamma$ -mediated activation of PKC $\alpha$  and a short pulse activation of the Ras/Raf/MAPK pathway resulting in cell adhesion and proliferation. FGF-induced signalling is over-ruled by the NCAM-mediated signals (Cavallaro *et al*, 2001; Francavilla *et al*, 2007).

the presence of E-cadherin, indicating that the levels of NCAM proteins determine its subcellular localization and thus its signalling qualities (Supplementary Figure S7). It is interesting to note that NCAM is a haplo-insufficient gene, indicating that NCAM gene dosage has a critical function in development and disease (Esni *et al*, 1999; Perl *et al*, 1999). Our results may provide a biochemical explanation for this gene dosage effect. The results also substantiate findings in neurons, where it has been demonstrated that NCAM140 localized in membrane compartments outside lipid rafts binds and stimulates FGFR through its fibronectin type III domains, which in turn activates PLC $\gamma$  and MAPK signalling pathways (Doherty and Walsh, 1996; Niethammer *et al*, 2002). In contrast, when situated within lipid rafts, NCAM associates with p59<sup>Fyn</sup> and activates FAK kinase-mediated signalling (Beggs *et al*, 1997; Niethammer *et al*, 2002).

Apparently, NCAM expression has an essential function in mesenchymal cell motility as characterized by the formation of  $\beta_1$ -integrin-dependent focal adhesions. We have shown earlier that the genetic ablation of NCAM gene expression results in the loss of  $\beta_1$ -integrin activation (Cavallaro *et al*, 2001) and that ablation of NCAM or  $\beta_1$ -integrin leads to reduced tumorigenicity of tumour cells (Kren *et al*, 2007). Here, we demonstrate that, after loss of E-cadherin function and gain of NCAM expression during EMT, phosphorylated FAK is stabilized and  $\beta_1$ -integrin-mediated cell spreading is enhanced. In contrast, in epithelial cells, FAK phosphorylation has a high turnover, very few focal adhesions are detected, and cell spreading is slow and largely  $\beta_1$ -integrin independent.

On the basis of the data presented, we conclude that the loss of E-cadherin, among many other molecular consequences, induces upregulated expression of the NCAM gene. As a result, increased levels of NCAM localize to lipid rafts and through p59<sup>Fyn</sup> induce the formation of focal adhesions and integrin-dependent mesenchymal cell migration and invasion. The correlation between the loss of E-cadherin and the gain of expression of NCAM and other Ig domain adhesion molecules in specific human cancer types and mouse models of carcinogenesis indicate that these molecular pathways have a critical function in malignant tumour progression and metastasis and, thus, warrant further investigation.

## Materials and methods

### Reagents and antibodies

Mouse NCAM-Fc (20  $\mu$ g/ml) was a gift from U Cavallaro (IFOM, Milano, Italy). TGF $\beta$ : R&D Systems (Abingdon, UK). Antibodies: anti- $\alpha$ -actin (Abcam, Cambridge, UK), anti-E-cadherin (for immunoblotting), anti-pY397FAK, anti-FAK, anti-p-paxillin, anti-pY528p59<sup>Fyn</sup> (BD Transduction Laboratories, Allschwil, Switzerland), anti-E-cadherin (for immunostaining; Zymed, San Diego, CA), anti-vinculin N-19 and anti-hNCAM 123C3 (Santa Cruz Biotechnology, Heidelberg, Germany), anti-vimentin clone V9, anti- $\beta$ -catenin and anti-hNCAM OB-11 (Sigma, Basel, Switzerland), anti- $\beta_1$ -integrin MAB2253Z (Millipore, Volketswil, Switzerland), anti-FGFR2 C-17, anti-cortactin 4F11, anti-PLC $\gamma$  and anti-p59<sup>Fyn</sup> (Upstate Biotechnology, Lake Placid, NY), anti-murine NCAM 5B8 (immunoblotting and immunofluorescence), anti-NCAM 13 (immunoprecipitation; BD Transduction Laboratories) and anti-N-cadherin (Takara Biomedicals, Tokyo, Japan).

### Cells and cell lines

A subclone of NMuMG cells (NMuMG/E9; hereafter NMuMG) expressing E-cadherin has been described earlier (Maeda *et al*, 2005). MDCKII, NMuMG, HEK293 and MCF7 cells were cultured in

DMEM supplemented with glutamine, penicillin, streptomycin and 10% FCS (Sigma). Oligonucleotides (Supplementary Table S1) were annealed and inserted into the pSUPER-retro-neo vector (Oligo-Engine, Seattle, WA) to generate pSUPER-Ecad-shRNA and pSUPER-Cont-shRNA. MCF7 and HEK293 cells stably transfected with pSuperRetro-Ecad-shRNA (shEcad) and pSuperRetro-mNCAM-shRNA (sh-cont) and MDCKII cells stably transfected with NCAM140 expression vectors were selected in G418. NMuMG-shSmad4 and NMuMG-shCont were obtained from P ten Dijke (Leiden University Medical Center, The Netherlands; Deckers *et al*, 2006). TGF $\beta$  treatment of NMuMG cells was performed without serum deprivation, and TGF $\beta$  was replenished every 3 days. MTfEcad cells were established from a mammary gland tumour isolated from an MMTV-Neu mouse (Muller *et al*, 1988) crossed with EcadF/F mice (Derksen *et al*, 2006). To establish the MTfEcad-Cre cell line, MTfEcad cells were infected with LZRSpBMN retroviral vector expressing Cre-IRES-GFP. After infection, GFP-expressing cells were sorted by FACS. hNCAM and mNCAM siRNAs were purchased from Invitrogen (Stealth siRNA duplex oligoribonucleotides; Supplementary Table S1). Transfections with LipofectAMINE RNAiMAX (Invitrogen) were performed according to the manufacturer's instructions. Total cell lysates, immunoblots and immunofluorescence experiments were performed as described earlier (Wicki *et al*, 2006). Depending on the species origin of antibodies, immunoblots were either probed sequentially or on multiple membranes. Adobe Photoshop has been used to excise the relevant portion of the immunoblots from the original scans of X-ray films exposed to chemiluminescence visualization of specific proteins, as indicated by black frames in the figures.

### Migration and invasion assays

Cell migration was determined in a modified two-chamber migration assay (pore size: 8  $\mu$ m; Falcon BD, Franklin Lakes, NJ). For invasion assays, membranes were coated with 20  $\mu$ l of a 2.5 mg/ml solution of Matrigel (Falcon BD). For both assays, 10<sup>5</sup> cells were seeded in 1% fetal calf serum/DMEM (Sigma) in the upper chamber, and the lower chamber was filled with 10% fetal calf serum/DMEM. After 24 h incubation at 37°C, cells in the upper chamber were carefully removed with a cotton swab and the cells that had traversed the membrane were fixed in 4% paraformaldehyde/HBS-Ca<sup>2+</sup>, stained with crystal violet (0.5% in 20% methanol) and counted.

### Cell spreading assay

To quantify cell spreading, cells were plated on a plastic culture dish, and 30 min after seeding the medium was changed to eliminate unattached cells. Cells were incubated at 37°C and counted in regular intervals in four independent experiments. In cases where  $\beta_1$ -integrin blocking antibodies were used, cells were incubated for 30 min with 100  $\mu$ g/ml mouse IgG or anti- $\beta_1$ -integrin antibodies prior to seeding.

### In vitro wounding assay

A scratch wound was generated using a 200  $\mu$ l pipette tip on confluent cell monolayers in a six-well culture plates in 10% serum containing DMEM medium (Sigma, St Louis, MO). Cells were then washed with fresh medium to remove floating cells. Microphotographs were taken at different time points.

### Quantitative RT-PCR

Total RNA was prepared using Trizol (Invitrogen), reverse transcribed with M-MLV reverse transcriptase RNase (H-) (Promega, Wallisellen, Switzerland), and transcripts were quantified by PCR using SYBR green PCR MasterMix (Applied Biosystems, Rotkreuz, Switzerland) and the primers indicated in Supplementary Table S1. Human or mouse riboprotein L19 primers were used for normalization. PCR assays were performed in triplicate, and fold induction was calculated against control-treated cell lines using the comparative C<sub>t</sub> method ( $\Delta\Delta C_t$ ).

### CAT assays

NMuMG cells were transfected with  $\Delta$ Nde and  $\Delta$ Ssp NCAM-CAT reporter constructs (Boras and Hamel, 2002) and treated with TGF $\beta$  for 6 days. CAT assays were performed using the CAT Enzyme Assay System (Promega). CAT activities were normalized relative to co-transfected control luciferase activities.

### Immunoprecipitations

Cells were lysed in RIPA-plus buffer. Equal amounts of proteins were incubated overnight with either mouse IgG or with anti-NCAM antibodies. Protein G sepharose beads (Sigma) were incubated with the immune complexes for 30 min, washed in cold lysis buffer and boiled in  $2 \times$  SDS-PAGE loading buffer.

### Flotation assays

Cells were lysed in cold lysis buffer for 30 min (1% Triton X-100, 25 mM Tris-HCl pH 7.5, 10% sucrose, 1 mM CaCl<sub>2</sub>, 1 mM MgCl<sub>2</sub> containing 1 mM NaF, 2 mM Na<sub>3</sub>VO<sub>4</sub>, 0.1 mM PMSF, 1 mM DTT and protease inhibitor cocktail), and isolation of Triton X-100-insoluble membrane fractions by sucrose gradient density centrifugation was performed as described (Oliiferenko *et al*, 1999).

### Histological analysis

Mice with a deletion of both E-cadherin alleles specifically in the  $\beta$ -cells of the islets of Langerhans were generated by crossing mice carrying E-cadherin alleles flanked by loxP sites (E-cadfl/fl; Derksen *et al*, 2006) with RipCre mice (Ahlgren *et al*, 1998). Mice were killed at the age of 56 days. The preparation of frozen tissue sections and immunofluorescence and immunohistochemical analysis was performed as described earlier (Perl *et al*, 1998; Wicki *et al*, 2006). In case of mouse-anti-mouse antibodies, background was reduced by additional blocking with the m.o.m. kit (Vector Laboratories, Burlingame, CA) according to the manufacturer's recommendations. The following primary antibodies were used at a 1:100 dilution: rat anti-mouse E-cadherin (Zymed), mouse anti-human E-cadherin (BD), anti-mouse NCAM 5B8 (a gift from U Cavallaro) and mouse anti-human NCA (OB11; Sigma). Stainings were evaluated on an AxioVert microscope and on a LSM 510 META confocal microscope (Zeiss, Oberkochen, Germany). Human cancer samples

were obtained with the consent of the Ethical Committee of the Kantons beider Basel.

### Statistical analysis

Statistical analysis and graphs were generated using the GraphPad Prism software (GraphPad Software Inc., San Diego, CA). All statistical analysis were done by unpaired, two-sided *t*-test. Normality testing was performed using the Kolmogorov-Smirnov test with Dallal-Wilkinson-Lillie for *P*-values.

### Supplementary data

Supplementary data are available at *The EMBO Journal* Online (<http://www.embojournal.org>).

### Acknowledgements

We are grateful to U Schmieder, H Antoniadis and R Jost for technical support. We thank A Fantozzi, M Cabrita and Adrian Zumsteg for critical input on the paper and sharing reagents. We thank MJ Wheelock and KR Johnson (University of Nebraska Medical Center, Omaha, USA), A-C Andres (Department of Clinical Research, University of Bern), G Orend (Institute for Biochemistry and Genetics, University of Basel), U Cavallaro (IFOM, Milano, Italy), P ten Dijke (Leiden University Medical Center, The Netherlands) and P Hamel (Faculty of Medicine, University of Toronto, Canada) for providing cell lines and important reagents. This study was supported by the EU-FP6 framework programme BRECOSM LSHC-CT-2004-503224, the Swiss Bridge Award, the Krebsliga Beider Basel (all GC), the Netherlands Organization for Scientific Research (NWO-VIDI 917.36.347 and NWO-VENI 916.56.135) and the Dutch Cancer Society (NKI 2002-2635) (AB and JJ).

### References

- Ahlgren U, Jonsson J, Jonsson L, Simu K, Edlund H (1998) Beta-cell-specific inactivation of the mouse *Ipfl/Pdx1* gene results in loss of the beta-cell phenotype and maturity onset diabetes. *Genes Dev* **12**: 1763-1768
- Beggs HE, Baragona SC, Hemperly JJ, Maness PF (1997) NCAM140 interacts with the focal adhesion kinase p125(fak) and the SRC-related tyrosine kinase p59(fyn). *J Biol Chem* **272**: 8310-8319
- Behrens J, Mareel MM, Van Roy FM, Birchmeier W (1989) Dissecting tumor cell invasion: epithelial cells acquire invasive properties after the loss of uvomorulin-mediated cell-cell adhesion. *J Cell Biol* **108**: 2435-2447
- Bhowmick NA, Ghiassi M, Bakin A, Aakre M, Lundquist CA, Engel ME, Arteaga CL, Moses HL (2001) Transforming growth factor-beta1 mediates epithelial to mesenchymal transdifferentiation through a RhoA-dependent mechanism. *Mol Biol Cell* **12**: 27-36
- Boras K, Hamel PA (2002) Alx4 binding to LEF-1 regulates N-CAM promoter activity. *J Biol Chem* **277**: 1120-1127
- Cavallaro U (2004) N-cadherin as an invasion promoter: a novel target for antitumor therapy? *Curr Opin Investig Drugs* **5**: 1274-1278
- Cavallaro U, Christofori G (2004) Cell adhesion and signalling by cadherins and Ig-CAMs in cancer. *Nat Rev Cancer* **4**: 118-132
- Cavallaro U, Niedermeyer J, Fuxa M, Christofori G (2001) N-CAM modulates tumour-cell adhesion to matrix by inducing FGF-receptor signalling. *Nat Cell Biol* **3**: 650-657
- Christofori G (2003) Changing neighbours, changing behaviour: cell adhesion molecule-mediated signalling during tumour progression. *EMBO J* **22**: 2318-2323
- Deckers M, van Dinther M, Buijs J, Que I, Lowik C, van der Pluijm G, ten Dijke P (2006) The tumor suppressor Smad4 is required for transforming growth factor beta-induced epithelial to mesenchymal transition and bone metastasis of breast cancer cells. *Cancer Res* **66**: 2202-2209
- Derksen PW, Liu X, Saridin F, van der Gulden H, Zevenhoven J, Evers B, van Beijnum JR, Griffioen AW, Vink J, Krimpenfort P, Peterse JL, Cardiff RD, Berns A, Jonkers J (2006) Somatic inactivation of E-cadherin and p53 in mice leads to metastatic lobular mammary carcinoma through induction of anoikis resistance and angiogenesis. *Cancer Cell* **10**: 437-449
- Doherty P, Walsh FS (1996) CAM-FGF receptor interactions: a model for axonal growth. *Mol Cell Neurosci* **8**: 99-111
- Esni F, Taljedal IB, Perl AK, Cremer H, Christofori G, Semb H (1999) Neural cell adhesion molecule (N-CAM) is required for cell type segregation and normal ultrastructure in pancreatic islets. *J Cell Biol* **144**: 325-337
- Francavilla C, Loeffler S, Piccini D, Kren A, Christofori G, Cavallaro U (2007) Neural cell adhesion molecule regulates the cellular response to fibroblast growth factor. *J Cell Sci* **120**: 4388-4394
- Friedl P, Wolf K (2003) Tumour-cell invasion and migration: diversity and escape mechanisms. *Nat Rev Cancer* **3**: 362-374
- Frixen UH, Behrens J, Sachs M, Eberle G, Voss B, Warda A, Lochner D, Birchmeier W (1991) E-cadherin-mediated cell-cell adhesion prevents invasiveness of human carcinoma cells. *J Cell Biol* **113**: 173-185
- Gavert N, Conacci-Sorrell M, Gast D, Schneider A, Altevogt P, Brabletz T, Ben-Ze'ev A (2005) L1, a novel target of beta-catenin signaling, transforms cells and is expressed at the invasive front of colon cancers. *J Cell Biol* **168**: 633-642
- Hanahan D (1985) Heritable formation of pancreatic beta-cell tumours in transgenic mice expressing recombinant insulin/simian virus 40 oncogenes. *Nature* **315**: 115-122
- Kren A, Baeriswyl V, Lehenbre F, Wunderlin C, Strittmatter K, Antoniadis H, Fassler R, Cavallaro U, Christofori G (2007) Increased tumor cell dissemination and cellular senescence in the absence of beta1-integrin function. *EMBO J* **26**: 2832-2842
- Lee JM, Dedhar S, Kalluri R, Thompson EW (2006) The epithelial-mesenchymal transition: new insights in signaling, development, and disease. *J Cell Biol* **172**: 973-981
- Maeda M, Johnson KR, Wheelock MJ (2005) Cadherin switching: essential for behavioral but not morphological changes during an epithelium-to-mesenchyme transition. *J Cell Sci* **118**: 873-887
- Mani SA, Yang J, Brooks M, Schwaninger G, Zhou A, Miura N, Kutok JL, Hartwell K, Richardson AL, Weinberg RA (2007) Mesenchyme Forkhead 1 (FOXC2) plays a key role in metastasis and is associated with aggressive basal-like breast cancers. *Proc Natl Acad Sci USA* **104**: 10069-10074



- Miettinen PJ, Ebner R, Lopez AR, Derynck R (1994) TGF-beta induced transdifferentiation of mammary epithelial cells to mesenchymal cells: involvement of type I receptors. *J Cell Biol* **127**: 2021–2036
- Muller WJ, Sinn E, Pattengale PK, Wallace R, Leder P (1988) Single-step induction of mammary adenocarcinoma in transgenic mice bearing the activated *c-neu* oncogene. *Cell* **54**: 105–115
- Niethammer P, Delling M, Sytnyk V, Dityatev A, Fukami K, Schachner M (2002) Cosignaling of NCAM via lipid rafts and the FGF receptor is required for neuritogenesis. *J Cell Biol* **157**: 521–532
- Oliferenko S, Paiha K, Harder T, Gerke V, Schwarzler C, Schwarz H, Beug H, Gunthert U, Huber LA (1999) Analysis of CD44-containing lipid rafts: recruitment of annexin II and stabilization by the actin cytoskeleton. *J Cell Biol* **146**: 843–854
- Perl AK, Dahl U, Wilgenbus P, Cremer H, Semb H, Christofori G (1999) Reduced expression of neural cell adhesion molecule induces metastatic dissemination of pancreatic beta tumor cells. *Nat Med* **5**: 286–291
- Perl AK, Wilgenbus P, Dahl U, Semb H, Christofori G (1998) A causal role for E-cadherin in the transition from adenoma to carcinoma. *Nature* **392**: 190–193
- Qin Y, Capaldo C, Gumbiner BM, Macara IG (2005) The mammalian Scribble polarity protein regulates epithelial cell adhesion and migration through E-cadherin. *J Cell Biol* **171**: 1061–1071
- Salon C, Moro D, Lantuejoul S, Brichon Py P, Drabkin H, Brambilla C, Brambilla E (2004) E-cadherin-beta-catenin adhesion complex in neuroendocrine tumours of the lung: a suggested role upon local invasion and metastasis. *Hum Pathol* **35**: 1148–1155
- Thiery JP (2003) Epithelial-mesenchymal transitions in development and pathologies. *Curr Opin Cell Biol* **15**: 740–746
- Thiery JP, Sleeman JP (2006) Complex networks orchestrate epithelial-mesenchymal transitions. *Nat Rev Mol Cell Biol* **7**: 131–142
- Wicki A, Lehenbre F, Wick N, Hantusch B, Kerjaschki D, Christofori G (2006) Tumor invasion in the absence of epithelial-mesenchymal transition: Podoplanin-mediated remodeling of the actin cytoskeleton. *Cancer Cell* **9**: 261–272